Valence band of $LiNi_xMn_{2-x}O_4$ and its effects on the voltage profiles of $LiNi_xMn_{2-x}O_4$/Li electrochemical cells

Yuan Gao* and K. Myrtle
Department of Physics, Simon Fraser University, Burnaby, British Columbia, Canada V5A 1S6

Meijie Zhang
Department of Physics, Simon Fraser University, Burnaby, British Columbia, Canada V5A 1S6
and Moli Energy (1990) Limited, Maple Ridge, British Columbia, Canada V2X 9E7

J. N. Reimers
Moli Energy (1990) Limited, Maple Ridge, British Columbia, Canada V2X 9E7

J. R. Dahn†
Department of Physics, Simon Fraser University, Burnaby, British Columbia, Canada V5A 1S6
(Received 17 May 1996; revised manuscript received 3 September 1996)

A high-voltage plateau at 4.7 V in $LiNi_xMn_{2-x}O_4$/Li electrochemical cells appears with the introduction of Ni into the $LiMn_2O_4$ spinel. The capacity of the 4.7-V plateau increases linearly at the expense of the 4.1-V plateau as x increases. Using ultraviolet photoelectron spectroscopy, we have studied the top of the valence band of $LiNi_xMn_{2-x}O_4$ for a series of samples with $0.0 \leqslant x \leqslant 0.5$. A component attributed to Ni $3d$ electrons was found at about 0.5-eV higher binding energy than the Mn $3d$ e_g electrons. We propose that the increased voltage of the 4.7-V plateau is due to the increased energy required to remove electrons from Ni $3d$ levels compared to Mn $3d$ e_g levels. [S0163-1829(96)03548-5]

INTRODUCTION

Lithium ion rechargeable batteries, which use lithium transition-metal oxides as the positive electrode and carbon as the negative electrode, not only have important applications in commercial electronics, but also are potential long-term candidates for powering emission-free vehicles.[1] Recently a new spinel, $LiNi_{0.5}Mn_{1.5}O_4$, prepared with a low-temperature sol-gel method, has been described by Amine *et al.*[2] In another paper of ours[3] we described the synthesis conditions and characterization of $LiNi_xMn_{2-x}O_4$ materials with solid-state techniques for use in Li-ion batteries. In this paper we study the change in the voltage profiles of $LiNi_xMn_{2-x}O_4$/Li cells and the change in the valence band of $LiNi_xMn_{2-x}O_4$ measured by ultraviolet photoelectron spectroscopy (UPS), as a function of the nickel content, x. We hope this study will shed light on why the nickel containing spinel has a voltage plateau at a higher voltage.

A rigid-band model is sometimes sufficient to describe the electron transfer when a Li atom intercalates within or deintercalates from the host material.[4] When a Li atom enters the host material, the Li atom donates its $2s$ electron to the host material to lower its energy (since the bands derived from Li^{2s} are normally well above the Fermi level), and the electron goes to an unoccupied state of the host. Similarly, when the Li^+ ion is removed from the host material, an electron is also removed from the topmost occupied state of the host.[4] Thus, as lithium is deintercalated, the Fermi level moves down with respect to the bands. In addition, the bands move up with respect to the vacuum, because of the removal of the compensating Li^+ ion. If the density of states is high and continuous, as it is for metallic systems, the upward motion of the bands balances the Fermi-level motion and, to the first, order, the position of the Fermi level with respect to the vacuum is unchanged, just as if a neutral atom is removed.[4] However, when the Fermi level moves through a gap in the density of states, large changes in the cell voltage can result as was shown in studies on $Li/Mo_{6-z}Ru_zSe_8$ electrochemical cells.[4] The rigid-band model has also been successfully applied to correlate the change of the voltage profiles on the Li insertion into different carbon materials and the change of the unoccupied electronic states as measured with x-ray-absorption spectroscopy.[5,6] In this paper we will also use the rigid-band model.

EXPERIMENT

$LiNi_xMn_{2-x}O_4$ samples were prepared with a sol-gel process as described in more detail in Ref. 3. Stoichiometric amounts of $Mn(CH_3COO)_2 4H_2O$ (SIGMA) and $Ni(NO_3)_2 6H_2O$ (BDH) were dissolved in distilled water and then mixed with LiOH (anachemia) solution to give $LiNi_xMn_{2-x}O_4$. A small amount of carbon black was added as a stabilizing agent. The resulting mixture was stirred for at least 1 h. The gel was further dried at 90 °C in air for about 4 h to reduce the volume. The gel was then heated in air at 400 °C for 24 h and then cooled to 100 °C in 1 h. The product was ground and then put back into the furnace in an alumina boat for the second heating. The second heating was also in air and was at 600 °C for 18 h. The samples were then cooled at 50 °C/h to room temperature.

Powder x-ray-diffraction measurements were made using a Siemens D5000 diffractometer equipped with a copper tar-

TABLE I. Summary of samples. The Ni content in $LiNi_xMn_{2-x}O_4$ is represented by x.

Sample	x	Reaction type	1st heating temperature (°C)	2nd heating temperature (°C)	a axis (Å)
*A*1	0.0	Solid state	750	750	8.2444
*N*6-1	0.1	Sol-Gel	400	600	8.2196
*N*6-2	0.2	Sol-Gel	400	600	8.2080
*N*6-3	0.3	Sol-Gel	400	600	8.1915
*N*6-4	0.4	Sol-Gel	400	600	8.1730
*N*6-5	0.5	Sol-Gel	400	600	8.1678

get x-ray tube and a diffracted-beam monochromator. All specimens were measured from 10° to 120° in scattering angle and each data collection took 15 h. No impurity peaks were detected in all of the samples except in $LiNi_{0.5}Mn_{1.5}O_4$, in which minute Li_xNi_{1-x} O ($x \leq 0.33$) peaks were present. The data was analyzed using Hill and Howard's[7] version of the Rietveld program. The goodness-of-fit (χ^2) and the Bragg R factor are better than 2% and 2.5%, respectively, for all of the refinement results. All of the samples are confirmed to have the same spinel structure as $LiMn_2O_4$ but with Ni substituting for Mn on 16*d* sites. No, Ni, or Mn was found on 8*a* sites. The lattice constants of the samples made here are included in Table I.

Electrochemical cells were made with the samples. Details and results have been described in Ref. 3.

Ultraviolet photoelectron spectroscopy (UPS) measurements were carried out with an ultrahigh vacuum surface analysis system. The base pressure of the system was better than 1×10^{-9} Torr. The pressure was typically $1\text{–}2\times10^{-8}$ Torr with the He lamp on. A windowless helium discharge lamp (vacuum generators) was used as the photon source. We were able to utilize helium discharge lines with 21.21- and 40.8-eV photon energies, respectively. A hemispherical electron energy analyzer (Perkin Elmer 10-360 Precision Energy Analyser) was used for the electron spectroscopy. The combined instrument resolution is believed to be 150 meV (using 10-eV pass energy). With the kinetic energy of a typical photoelectron in this study being 20–40 eV, a surface layer of the order of 10 Å is detected.[8] For UPS measurements, powder samples were pressed into pellets and sintered for mounting and grounding purposes. The pressed pellets were heated to 750 °C for 18 h and then slow cooled to room temperature. The cooling rate was 25 °C/h from 750 °C to 500 °C, and 50 °C/h from 500 °C downwards. The slow cooling from 750 °C to 500 °C was to ensure adequate intake of oxygen by the pellet samples. The sample pellet was held with a piece of copper foil to the stainless-steel holder and adequate grounding was ensured during the UPS measurement.

RESULTS AND DISCUSSION

Review of electrochemical results presented in Ref. 3

Electrochemical results for samples with $x=0.0$, 0.1, 0.2, 0.3, 0.4, and 0.5 have been presented in Ref. 3. For $x=0$, the voltage curve of $Li/LiNi_xMn_{2-x}O_4$ cells has a plateau at 4.1 V as Li is removed from the host (as the cells are charged). For $x=0.5$, the 4.1 V plateau is absent and a 4.7-V plateau appears. For intermediate values of x, the 4.1-V plateau has a length proportional to $1-2x$ and the 4.7-V plateau has length proportional to $2x$ (3).

Undoubtedly the appearance of the high-voltage plateau is due to the nickel ions. It has been shown by Amine *et al.* with x-ray photoelectron spectroscopy (XPS) that the oxidation state of Ni in $LiNi_{0.5}Mn_{1.5}O_4$ is 2.[2] Therefore we can reasonably assume that the nickel ions in the whole series of $LiNi_xMn_{2-x}O_4$ materials with $0\leqslant x\leqslant 0.5$ are also Ni^{2+}. With this assumption and charge neutrality one can write $LiNi_xMn_{2-x}O_4$ as $LiNi_x^{2+}Mn_{1-2x}^{3+}Mn_{1+x}^{4+}O_4$. We propose that it is the oxidation of Mn^{3+} to Mn^{4+} on the 4.1-V plateau and the oxidation of Ni^{2+} to Ni^{4+} on the 4.7-V plateau when Li is removed. This means that the capacity in the 4.1-V plateau is $(1-2x)$ Li atoms per formula unit and the capacity in the 4.7-V plateau is $2x$ Li atoms per formula unit as observed in Ref. 3.

The nearest-neighbor oxygen environment around each Li atom is independent of x since the spinel structure is maintained. In earlier work on $Li/Mo_xSe_zS_{8-z}$ electrochemical cells, Selwyn *et al.*[9] showed that the voltage profiles, which are plateaus at 2.5 V for $z=0$ and at 2.1 V for $z=8$, become strongly sloped between these voltages for intermediate values of z. In this material, the Li atoms reside in sites with eight anion neighbors and the local environment of the Li atom exhibits a statistical variation when z is not 0 or 8. That is, one finds Li atoms with 0, 1, 2, 3, ... sulfur and 8, 7, 6, 5, ... selenium neighbors when z is not 0 or 8 with a probability that depends on z. The binding energy of the Li atom to the host is strongly affected by its local environment and a range of binding energies results, leading to sloping voltage profiles. In $LiNi_xMn_{2-x}O_4$, the situation is different, and mimics that in $Mo_{6-z}Ru_zSe_8$,[4] where there is a *sharp* voltage change between two plateaus. In these two materials, the *second* neighbor (i.e., the cation, not the anion) to the lithium varies and local effects are thought not to be dominant. It is the changes to the electronic structure that are most important. The rigid-band model was used to explain the changes in the voltage profiles of $Li/Mo_{6-z}Ru_zSe_8$ cells with z, and we will use it here.

Photoelectron spectroscopy

It is difficult to understand why the plateau in the Ni-doped spinel is at a higher voltage without a knowledge of the electron valence band of the material. The voltage of the $LiNi_xMn_{2-x}O_4/Li$ electrochemical cell equals the difference between the chemical potentials of the Li atom in $LiNi_xMn_{2-x}O_4$ and in Li metal. In other words, the binding energy of the Li atom consists of the binding energy of the Li^+ ion and the binding energy of the electron. When a Li atom is removed from $LiNi_xMn_{2-x}O_4$ on charge, one removes a Li^+ ion from an 8*a* site and an electron from the valence band of $LiNi_xMn_{2-x}O_4$. Since the introduction of the Ni ions into the $LiMn_2O_4$ spinel does not change the *nearest* neighbors to the lithium, it is very unlikely that there is a $\sim$0.6-eV jump in the Li^+ binding energy caused by replacing some Mn with Ni, as argued above. Therefore it is

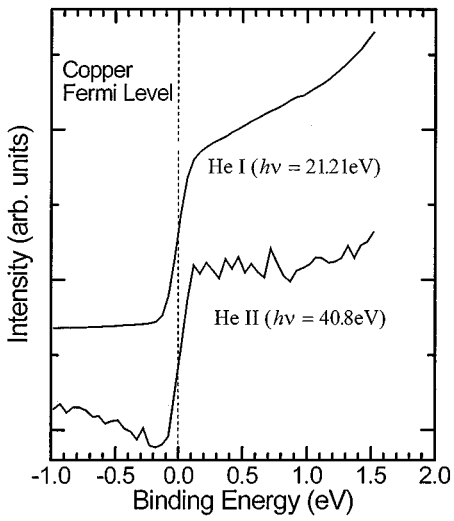

FIG. 1. UPS spectra measured on a copper foil with He I and He II lines, respectively. The Cu Fermi level, which is indicated by the dotted line, is used to define the binding-energy zero in all of our spectra.

crucial to see how the valence-band changes in $LiNi_xMn_{2-x}O_4$ as a function of x.

The valence band of $LiNi_xMn_{2-x}O_4$ samples was measured with ultraviolet photoelectron spectroscopy (UPS) using a He discharge lamp. Two discharge lines with different photon energies can be utilized with our He lamp, namely, $h\nu = 21.21$ eV (He I) and $h\nu = 40.8$ eV (He II). Figure 1 shows the UPS spectra taken with He I and He II photons on the copper foil of the pellet holder. A very sharp Fermi edge can be seen in both spectra which confirms that the overall instrument resolution is indeed better than 150 meV. From now on we use the Fermi level measured on copper as the binding-energy zero for all our UPS spectra.

Figure 2 shows the UPS spectra of sample $A1(x = 0.0)$ measured with two different photon energies. The sloping backgrounds at high binding energy in the spectrum measured with He I is due to the low-kinetic-energy secondary electrons generated by collisions of photoelectrons with the solid, which are avoided with the use of He II because of the higher photon energy. Valence bands of manganese monoxide and other transition-metal monoxides have been extensively studied both theoretically[10–12] and experimentally.[12–14] In these transition metal monoxides, the transition metal is also octahedrally coordinated by the oxygen atoms, just like in the spinel. This enables us to label most of the prominent features in Fig. 2. Features *a* and *b* can be attributed to the e_g and t_{2g} components of Mn $3d$, respectively.[12,13] Feature *c* is mostly O $2p\pi$ bonded to the metal $3d$.[13] Feature *d* is also from O $2p$.[12,13] Feature *e* is the so-called satellite peak, the origin of which has been the subject of debate for years.[13,14] We are unclear about the origin of feature *f*.

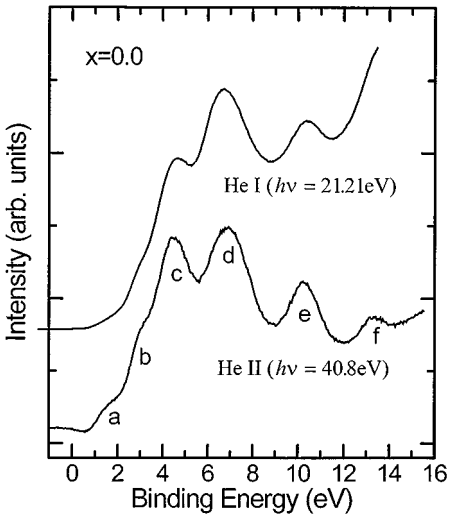

FIG. 2. UPS spectra of sample Al ($x = 0.0$) measured with He I and He II lines, respectively.

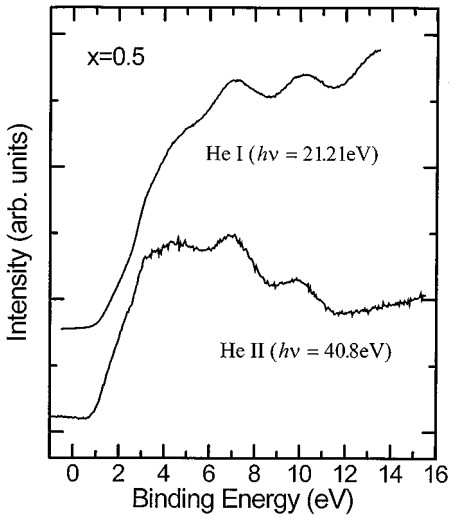

FIG. 3. UPS spectra of sample $N6\text{-}5(x = 0.5)$ measured with He I and He II lines, respectively.

The cross section of O $2p$ decreases and the cross section of Mn $3d$ increases when the photon energy changes from 21.21 to 40.8 eV.[15] As shown in Fig. 2, the intensities of features *d* and *e* do not change much when the photon energy is reduced from 40.8 to 21.21 eV, suggesting that they are mostly of O $2p$ character. The intensities of features *a* and *b* decrease very much from the He II spectrum to the He I spectrum. Feature *a* is almost invisible in the He I spectrum because of this cross-section reduction. This shows that features *a* and *b* are indeed mostly of Mn $3d$ character. Feature *c* has mostly O $2p$ character with some Mn $3d$ character,[13] and does not decease as much as features *a* and *b* with the same photon energy change.

Figure 3 shows the UPS spectra of sample $N6-5$ $(x = 0.5)$, taken with two different photon energies. A similar relative intensity change is observed from one photon energy to the other, namely, the features near the top of the valence band are enhanced with $h\nu = 40.8$ eV. The feature at 3.4 eV that can be attributed to the Mn $3d$ t_{2g} level (labeled as feature *b* in Fig. 2) is now stronger in Fig. 3. We will discuss this more later once we have a clearer picture of the Ni $3d$ levels.

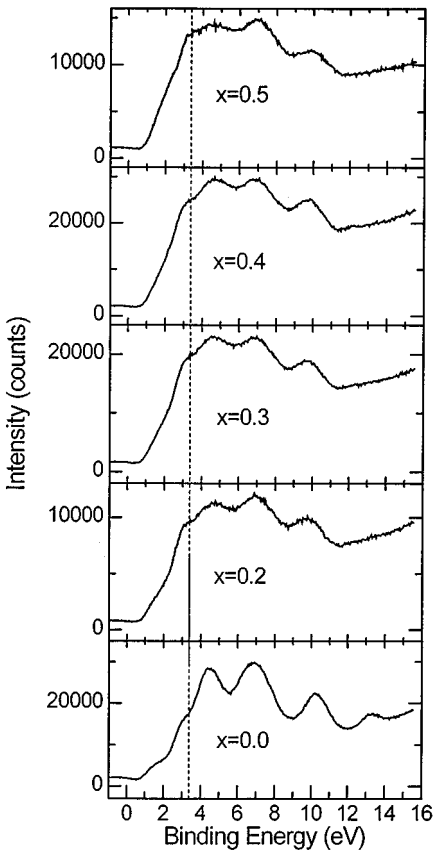

FIG. 4. UPS spectra for a series of samples measured with the He II line (photon energy = 40.8 eV). The dotted line indicates where the spectra in Fig. 5 were normalized.

Figure 4 shows UPS spectra of samples with different x, taken with 40.8-eV photon energy. Since we are primarily interested in the energy alignment of the transition metal $3d$ levels, we will compare the spectra very carefully in the region of the top of the valence band (binding energy less than 3.5 eV). First we normalize all the spectra at 3.4-eV binding energy and plot them in Fig. 5. The dashed line in

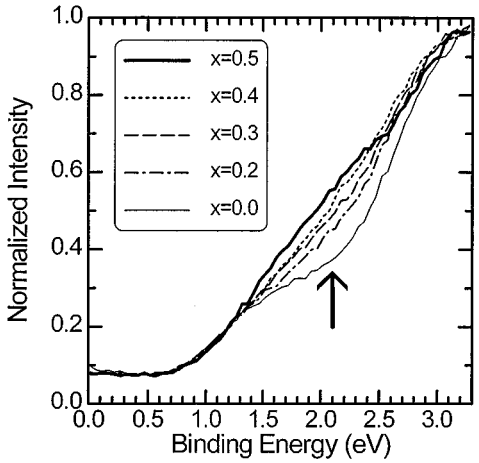

FIG. 5. A comparison of the top of the valence band of the UPS spectra shown in Fig. 7. The spectra were all normalized at 3.4-eV binding energy.

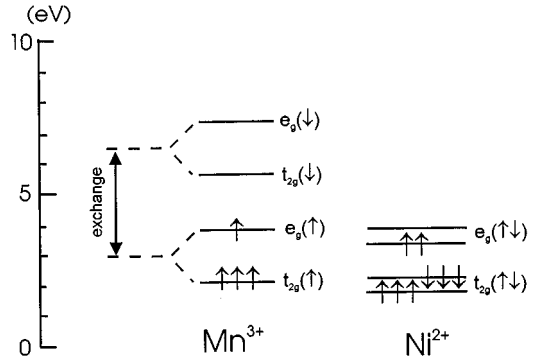

FIG. 6. A schematic diagram showing the $3d$ levels of Mn^{3+} and Ni^{2+} in $LiNi_xMn_{2-x}O_4$. The four $3d$ electrons of Mn^{3+} and the eight $3d$ electrons of Ni^{2+} are schematically shown in the occupied states by $\uparrow$ and $\downarrow$. A scale bar is also shown on the left.

Fig. 4 indicates where the normalization was made for the plot in Fig. 5. With this normalization, Fig. 5 illustrates the relative change of the energy distribution of the density of states of the metal $3d$ levels above Mn $3d$ t_{2g}, as a function of x. As shown in Fig. 5, there is a component centered at about 2.1 eV (indicated by an arrow) which increases with increasing Ni content x. Clearly, this component is related to Ni.

In order to understand what we have observed, we now look at the $3d$ levels of Mn and Ni octahedrally coordinated with oxygen. Mn $3d$ has a relatively large exchange splitting ($0.26R_y \cong 3.5$ eV) and the $3d$ levels are further split by the crystal field into e_g and t_{2g} levels.[12] This is shown schematically in Fig. 6. For Mn^{3+}, all four $3d$ electrons will be with the majority spin (represented by $\uparrow$), and three electrons will be on $t_{2g}(\uparrow)$ and one electron will be on $e_g(\uparrow)$. Accordingly, the feature at about 1.5-eV binding energy in the spectrum of sample with $x=0.0$ (Figs. 2 and 5) is from $e_g(\uparrow)$ and the feature at about 3.4-eV binding energy is from $t_{2g}(\uparrow)$.[12,13] For Ni, the situation is different. The exchange splitting for both Co and Ni is much smaller than that of Mn.[12,16] Furthermore, van Elp and coworkers have shown that the ground state of Co^{3+} ($3d^6$ configuration) in $LiCoO_2$ has a low spin configuration instead of a high spin configuration as in the case of CoO.[16] In the low spin configuration, Co^{3+} has two nearly degenerate $t_{2g}(\uparrow\downarrow)$ and $e_g(\uparrow\downarrow)$ levels and all six Co $3d$ electrons are on the same nearly degenerate $t_{2g}(\uparrow\downarrow)$ level.[16] They attribute this to the fact that the reduced Co-O distance in $LiCoO_2$, as compared to that in CoO, increases the crystal field, which makes the low spin configuration more favorable.[16] The exchange splitting of Ni is even smaller than that of Co ($0.05R_y \cong 0.7$ eV for Ni in NiO and $0.16R_y \cong 2.1$ eV for Co in CoO).[12] It is very likely that Ni^{2+} also favors the low spin configuration in $LiNi_xMn_{2-x}O_4$ since it also has a small exchange interaction and a small Ni-O distance (2.04 Å for $x=0.5$). Actually it has been shown with magnetic measurements that Ni has a low spin configuration in $LiNiO_2$.[17] In the low spin configuration, the $3d^8$ electron configuration of Ni^{2+} will have six electrons on the nearly degenerate $t_{2g}(\uparrow\downarrow)$ level and two electrons on the nearly degenerate $e_g(\uparrow\downarrow)$ level. This is schematically illustrated in Fig. 6.

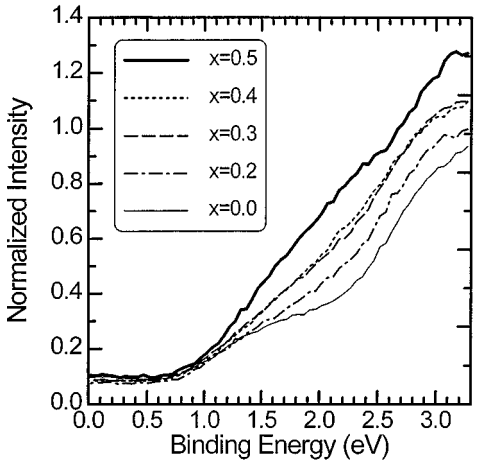

FIG. 7. A comparison of the top of the valence band of the UPS spectra shown in Fig. 4. The spectra were all normalized to the background at 15.0-eV binding energy.

The exact alignment of the $t_{2g}(\uparrow\downarrow)$ and $e_g(\uparrow\downarrow)$ levels of Ni^{2+} with the $t_{2g}(\uparrow)$ and $e_g(\uparrow)$ levels of Mn^{3+} is not known in the literature. However, from our UPS spectra of $LiNi_xMn_{2-x}O_4$, we feel it is likely that $t_{2g}(\uparrow\downarrow)$ of Ni^{2+} is very close to $t_{2g}(\uparrow)$ of Mn^{3+}, which is at about 3.4 eV. The component centered at 2.1 eV that increases with the Ni content (Fig. 5) is most likely to be from $e_g(\uparrow\downarrow)$ of Ni^{2+}. Unlike core levels, the valence levels tend to be more delocalized, and therefore hybridization between Ni and Mn $3d$ states is possible. Nevertheless, the feature at 2.1 eV clearly arises from the Ni content in $LiNi_xMn_{2-x}O_4$. Hence we continue using the labels of Ni $t_{2g}(\uparrow\downarrow)$ and $e_g(\uparrow\downarrow)$ for identification even though there is some degree of mixing with other states.

Figure 7 shows the top of the valence-band region of the UPS spectra normalized with the spectrum background at 15-eV binding energy, in order to compare the relative intensity in the metal $3d$ region. As shown in Fig. 7, the increase of the component centered at 2.1 eV shows the same trend as in Fig. 5, which is consistent with the Ni $e_g(\uparrow\downarrow)$ assignment. The intensity at 3.4 eV also increases with x. This is presumably because there are more electrons in Ni $t_{2g}(\uparrow\downarrow)$ than in Mn $t_{2g}(\uparrow)$.

Relation of photoelectron spectroscopy results to electrochemical results

Now that we have a picture of the $3d$ levels of Mn and Ni in $LiNi_xMn_{2-x}O_4$, we attempt to understand why the plateau moves from 4.1 to 4.7 V in $LiNi_xMn_{2-x}O_4$/Li cells as x increases. As we stated earlier, the 4.1-V plateau corresponds to oxidation of Mn^{3+} to Mn^{4+} and the 4.7-V plateau corresponds to oxidation of Ni^{2+} to Ni^{4+} when Li is removed from $LiNi_xMn_{2-x}O_4$. As an electron is removed from Mn^{3+}, it is removed from Mn $e_g(\uparrow)$ which has an electron binding energy at around 1.5–1.6 eV, and this is on the 4.1-V plateau. When there are no more electrons left on Mn $e_g(\uparrow)$ (all Mn are Mn^{4+} now), electrons are removed from Ni $e_g(\uparrow\downarrow)$ which has an electron binding energy of about 2.1 eV, and the voltage plateau moves up to 4.7 V because of the increased energy needed to remove electrons.

There still seems to be a problem. The UPS intensity at around 1.5-eV binding energy does not decrease with increasing Ni content, even when x reaches 0.5. However, the surface of the material can be more reduced, namely, the cations can have more electrons on them simply because there are not as many oxygen atoms around them on the surface. UPS can only detect about 10 Å on the surface.[8] Therefore it is possible for a coexistence of Mn^{3+} and Ni^{2+} on the surface even when x reaches 0.5. This might explain why the capacity of the 4.1-V plateau is not really zero even with $x=0.5$ (see Ref. 3). Nevertheless, the detection of a component in the valence band of $LiNi_xMn_{2-x}O_4$ that is related to Ni and has a higher binding energy than that of Mn $e_g(\uparrow)$, is very suggestive of the origin of the 4.7-V plateau in $LiNi_xMn_{2-x}O_4$/Li electrochemical cells.

CONCLUSION

In conclusion, we have carefully measured the voltage profiles of $LiNi_xMn_{2-x}O_4$/Li electrochemical cells. The high-voltage plateau (4.7 V) increases linearly at the expense of the low-voltage plateau (4.1 V) with increasing nickel content. Using ultraviolet photoelectron spectroscopy, we can compare the top of the valence band of $LiNi_xMn_{2-x}O_4$ with samples having a range of $0 \leqslant x \leqslant 0.5$. A component that can be attributed to Ni $3d$ electrons was found at about 0.5-eV-higher binding energy that the Mn $3d e_g(\uparrow)$ electrons. This explains why the oxidation state of Ni is $+2$ in the $LiNi_xMn_{2-x}O_4$ system, because Mn just dumps its $3d$ $e_g(\uparrow)$ electrons to the lower Ni $3d$ $e_g(\uparrow\downarrow)$ level. We propose that the increased voltage of the plateau corresponding to Ni, is due to the increased energy it requires to remove electrons from Ni $3d$ levels.

ACKNOWLEDGMENT

The financial support of the Natural Science and Engineering Research Council of Canada through the Strategic grants program is acknowledged.

*Current address: FMC Corporation, Lithium Division, Highway 161, Box 795, Bessemer City, North Carolina 28016.

†Author to whom correspondence should be addressed. Permanent address: Department of Physics, Dahlhousie University, Halifax, Nova Scotia, Canada B3H 3J5.

[1] See, for example, K. Brandt, Solid State Ion. **69**, 173 (1994); *Lithium Batteries, New Materials, Developments and Perspectives*, edited by G. Pistoia (Elsevier, New York, 1994).

[2] K. Amine, H. Tukamoto, H. Yasuda, and Y. Fujita, *Extended Abstracts 95-2, Electrochemical Society Fall Meeting 1995, Chicago* (The Electrochemical Society, Pennington, NJ, 1995), Abstract no. 70, p. 114.

[3] Qiming Zhong, Arman Bonakdarpour, Meijie Zhang, Yuan Gao, and J. R. Dahn, J. Electrochem. Soc. (to be published).

[4] W. R. McKinnon, in *Solid State Electrochemistry*, edited by P. G. Bruce (Cambridge University Press, Cambridge, 1995), Chap. 7, pp. 163–198.

[5] J. R. Dahn, J. N. Reimers, T. Tiedje, Y. Gao, A. K. Sleigh, W. R.

McKinnon, and S. Cramm, Phys. Rev. Lett. **68**, 835 (1992).
[6] B. M. Way and J. R. Dahn, J. Electrochem. Soc. **141**, 907 (1994); J. R. Dahn, J. N. Reimers, A. K. Sleigh, and T. Tiedje, Phys. Rev. B **45**, 3773 (1992).
[7] R. J. Hill and C. J. Howard, J. Appl. Crystallogr. **18**, 173 (1985).
[8] D. R. Penn, Phys. Rev. B **13**, 5248 (1976); S. Tanuma, C. J. Powell, and D. R. Penn, Acta Phys. Pol. A **81**, 169 (1992). See also, for example, A. Zangwill, *Physics at Surfaces* (Cambridge, New York, 1990).
[9] L. S. Selwyn, W. R. McKinnon, J. R. Dahn, and Y. LePage, Phys. Rev. B **33**, 6405 (1986).
[10] L. F. Mattheiss, Phys. Rev. B **5**, 290 (1972); **5**, 306 (1972).
[11] A. Fujimori, F. Minami, and S. Sugano, Phys. Rev. B **29**, 5225 (1984); A. Fujimori and F. Minami, *ibid.* **30**, 957 (1984).
[12] T. Oguchi, K. Terakura, and A. R. Williams, Phys. Rev. B **28**, 6443 (1983); J. Appl. Phys. **55**, 2318 (1984); K. Terakura, T. Oguchi, A. R. Williams, and J. Kübler, Phys. Rev. B **30**, 4734 (1984).
[13] R. J. Lad and V. E. Henrich, Phys. Rev. B **38**, 10 860 (1988).
[14] Shin-Puu Jeng, R. J. Lad, and V. E. Henrich, Phys. Rev. B **43**, 11 971 (1991).
[15] J. J. Yeh and I. Lindau, At. Data Nucl. Data Tables **32**, 1 (1985).
[16] J. van Elp, J. L. Wieland, H. Eskes, P. Kuiper, G. A. Sawatzky, F. M. F. de Groot, and T. S. Turner, Phys. Rev. B **44**, 6090 (1991).
[17] K. Hirakawa, H. Kadowaki, and K. Ubukoshi, J. Phys. Soc. Jpn. **54**, 3526 (1985); K. Hirakawa and H. Adowaki, Physica **136B**, 335 (1986).